Efficient capture of phosphate from aqueous solution using acid activated akadama clay and mechanisms analysis

Ying Wang, Hui He, Nan Zhang, Kazuya Shimizu, Zhongfang Lei and Zhenya Zhang

ABSTRACT

In this study, akadama clay, a kind of volcano ash, was activated with sulfuric acid and then evaluated for the adsorption of phosphate from aqueous solution via batch experiments. The effects of adsorbent dose, initial pH and co-existing anions on phosphate removal by natural akadama clay and acid-activated akadama clay were investigated. Based on the pH effect, the modified adsorbent could efficiently capture phosphate over a wider pH range of 3.00–6.00 than natural akadama clay. Competitive anions showed negative effects on the phosphate adsorption, especially citrate and carbonate. The adsorption process followed the pseudo-second-order kinetic equation and the intra-particle diffusion. Langmuir isotherm model was found to fit the data better than Freundlich model, and the maximum adsorption capacities of phosphate onto the natural akadama clay and acid-activated akadama clay were 5.88 and 9.19 mg/g, respectively. Furthermore, thermodynamic studies confirmed that the adsorption of acid-activated akadama clay was a spontaneous process. The mechanisms of phosphate adsorption on the clay could be ascribed to electrostatic attraction and ligand exchange. These results suggest that after modification, acid-activated akadama clay could be used as a promising adsorbent for phosphate removal from wastewater in real application and then further used as fertilizers.

Key words | activated akadama clay, adsorption, mechanisms, phosphate, sulfuric acid

Ying Wang
Hui He
Nan Zhang
Kazuya Shimizu
Zhongfang Lei
Zhenya Zhang (corresponding author)
Graduate School of Life and Environmental Sciences,
University of Tsukuba,
1-1-1, Tennodai, Tsukuba, Ibaraki 305-8572, Japan
E-mail: *zhang.zhenya.fu@u.tsukuba.ac.jp*

INTRODUCTION

Water pollution is attracting more and more attention in developing countries, especially now in China. Among these pollutions, eutrophication is triggered largely by excess phosphorus (P) in water bodies such as estuaries and lakes, resulting in outbreak of algal blooms, aquatic life loss and poor water quality, further leading to decrease in biological diversity and increase in potential health risk to human beings (Diaz & Rosenberg 2008). The concentration of P in lakes and reservoirs has been reported to be about 0.03 mg/L, or 0.05–0.1 mg-P/L in streams (U.S. Environmental Protection Agency 1996), which is considered to be the minimum margin concentration of phosphate to induce eutrophication. It is well known that the dominant sources of phosphorous as phosphate form come from municipal and industrial wastewaters. Meanwhile, an approximate concentration of total phosphate (TP) is 6–25 mg-P/L in a typical raw municipal wastewater, with ortho-phosphate of 4–15 mg-P/L as the principal form of phosphate (Henze *et al.* 2008). Consequently, before being discharged into natural water bodies like lakes and rivers, the wastewaters should be properly treated by some applicable technologies to remove phosphate efficiently in order to meet the effluent standard.

The main phosphate removal and recovery technologies include ion exchange, biological methods, crystallization and adsorption. Among these technologies, adsorption is a promising method due to some advantages superior to others, like minimum sludge disposal, flexibility and simplicity of design, easy control, low-cost and the possibility of phosphate recovery. Although many adsorbents have been developed from fly ash, iron oxides, nano-particles, activated carbon and functionally modified adsorbents, most of them

doi: 10.2166/wst.2018.441

are obtained from complicated preparation processes at high-cost, low-efficiency or unsatisfactory adsorption capabilities. Hence, new adsorbents with low cost and high efficiency are still of great importance.

Akadama clay (AC), a kind of volcanic soil, is abundant in Japan. AC is widely used as soil medium since it has high osmotic, strong impounding and water draining properties. Up to now, AC has been investigated as an efficient adsorbent to remove As (Chen *et al.* 2010), Cs (Ding *et al.* 2014) and Cr (VI) (Zhao *et al.* 2015) from aqueous solutions. To the best of our knowledge, up to the present, little information is available on the removal of phosphate by using AC or modified AC under different adsorption conditions.

Acid activation has long been used to produce sorbents for certain practical applications. Previously, Ye *et al.* pointed out that acid activation can clean the effective adsorption sites on adsorbent surface, and the addition of acid solution helps to partially dissolve minerals and increase surface protonation (Ye *et al.* 2016). Sulfuric acid-modified fly ash has been reported to have a greater phosphate adsorption capacity due to the dissolution of the amorphous siliceous spherical particulates (Xu *et al.* 2010). However, it is unknown that whether phosphate removal capacity could be enhanced by acid activation on akadama clay, let alone the mechanisms involved. In this study, the sorption performance of natural AC (NAC) and H_2SO_4 activated AC (HAC) were compared and evaluated based on the batch adsorption experiments. The effects of contact time, solution pH, initial P concentration, and adsorbent dosage on P removal efficiency were investigated. The adsorption kinetics, isotherm models and thermodynamic studies were carried out to evaluate the adsorption process. The mechanisms of P removal onto NAC and HAC were also analyzed.

MATERIALS AND METHODS

Chemicals and materials

All chemical reagents (KH_2PO_4, H_2SO_4, NaOH, HCl, NaCl, $NaNO_3$, Na_2SO_4, Na_2CO_3, $Na_3C_6H_5O_7$) were of analytical grade and were supplied by Wako Pure Chemical Industries. The natural akadama clay (NAC) employed in the present study was obtained from the Makino Store, Kiyosu, Japan. It was crushed and sieved to powder smaller than 105 μm, then dried in an oven (EYELAWFO-700, Japan) at 105 °C for 24 h.

Preparation of the adsorbent

The acid-activated akadama clay (HAC) was prepared by the following procedures. 5 g of dried NAC was added to 50 mL 0.1 M H_2SO_4 solution in a flask and mixed for 24 h under vigorous stirring at ambient temperature (25 ± 2 °C) in a thermostatic shaker. After centrifuged, the resultant solid was washed several times with deionized water to neutral pH and finally dried at 105 °C. The collected HAC was ground and passed through a 105 μm mesh sieve, then used in the following phosphate removal experiments.

Batch adsorption experiments

A stock solution with a concentration of 500 mg/L phosphate was prepared by dissolving KH_2PO_4 (analytical grade) in deionized water and diluted to the desired concentration in the following experiments. Each experiment was conducted in triplicate under identical conditions with average values being used.

In the batch adsorption experiments, a series of equilibrium tests were conducted to investigate the phosphate adsorption behaviors of NAC and HAC. 0.1 M HCl or NaOH solution was used to adjust the solution pH. The phosphate adsorption capacity q_e (mg/g) and removal efficiency R (%) were calculated according to the following equations:

$$q_e = \frac{(C_0 - C_e)}{m} \times V \quad (1)$$

$$R(\%) = \frac{(C_0 - C_e)}{C_0} \times 100 \quad (2)$$

where C_0 (mg/L) and C_e (mg/L) are the initial and equilibrium phosphate concentrations in the solution, m (g) is the dry weight of the adsorbent, and V (L) is the volume of the tested solution.

For adsorption kinetic studies, 1 g of the NAC or HAC was mixed with 200 mL of phosphate solution (20 mg/L) at pH of 6.90 ± 0.10 in a flask and shaken under 100 rpm. Samples were taken at designated intervals (0–540 min) and filtered through 0.22 μm membrane filter before the measurement of the residual phosphate concentration. The other experiments were carried out in 50 mL plastic centrifuge tubes containing 40 mL of 20 mg/L phosphate solution in a shaker at ambient temperature (25 ± 2 °C) for 24 h to better understand the behavior of the adsorbent. The coexisting anions experiments were conducted using

commonly coexisting anions in phosphate-containing wastewaters including 0.01 M nitrate ($NaNO_3$), sulfate (Na_2SO_4), carbonate (Na_2CO_3) and citrate ($Na_3C_6H_5O_7$) (Wang *et al.* 2016). The detailed experimental conditions in this study are summarized in Table S1.

Analytical methods

The elemental composition and surface morphology of the adsorbent were obtained by energy dispersive X-ray spectroscopy (EDS) with 30 kV accelerating voltage and field emission scanning electron microscope (FE-SEM, S-4800; Hitachi Hitec Corp., Japan) at 5 kV accelerating voltage after Pt-Pd being coated with an ion sputter coater (E-1030; Hitachi Ltd., Japan). The mineralogical phase characterization of the clay was carried out by quantitative X-ray diffraction (XRD) (D2 phazer; Bruker Analytik, Germany) with Cu Kα ($\lambda = 1.54$ Å) radiation in the 2θ range of 5–80° at 30 kV and 10 mA. The Fourier transform infrared (FT-IR) spectrum of the samples were performed on Nicolet iS5 with a resolution of 4 cm^{-1} by using attenuated total reflectance (ATR) technique (Nicolet Biomedical Inc., USA) in the wavenumber range of 400–4,000 cm^{-1}. The Brunauer–Emmett–Teller (BET) surface area and total pore volume were analyzed based on N_2 adsorption–desorption isotherms by using BELSORP-mini (Microtrac BEL Inc, Japan). pH was measured with a pH meter (Mettler Toledo SG8, Switzerland).

The concentration of phosphate was determined with a well-established molybdate blue spectrophotometric method (Chen *et al.* 2016). In brief, a certain amount of ascorbic acid solution was added to a graduated centrifuge tube which contained sample, and about 30 seconds later a certain amount of molybdate solution was added into the centrifuge tube and mixed thoroughly. After standing for 15 min at room temperature, a blue color complex was formed with the absorption being measured at a wavelength of 700 nm using a UV spectrophotometer (UV-1800, Shimadzu Corp., Japan).

RESULTS AND DISCUSSION

Characterization

The SEM images (Figure 1) of NAC and HAC were taken before and after adsorption of phosphate, respectively. For NAC (Figure 1(a)), the random distribution of small particles between flat and coarse areas implies the wide existence of amorphous particles but the surface is relatively smooth. As for HAC (Figure 1(b)), SEM may provide visual evidence of the effect of H_2SO_4 on the clay surface erosion, and its surface reflected a coarse exterior probably due to the removal of some acid-soluble salts (Huang *et al.* 2008). After adsorption, the particles of NAC aggregated together as shown in Figure 1(c), while HAC became compact and smooth (Figure 1(d)), revealing the surface structure was significantly changed after phosphate adsorption. As a result, the morphological changes of SEM images after modification and adsorption are attributable to the changes in their particle size and their agglomeration after phosphate adsorption (Zhao *et al.* 2015).

Generally, octahedral cations such as Al^{3+}, Fe^{3+}, and Mg^{2+} in clay can be depleted by treating clay minerals with acid (Novaković *et al.* 2008). From the EDS elemental analysis in this study (Table S2), the weight percentages of Al and Fe in the surface increased after acid modification, most probably due to the fact that the inner layer of Al and Fe migrated outward (Zhao *et al.* 2015). Definitely, the occurrence in phosphate content after HAC adsorption of phosphate was contributed by phosphate adsorption onto the clay surface.

FTIR spectra of the NAC and HAC are shown in Figure 2(a). The broad absorption band of 3,230–3,450 cm^{-1} with the peak around 3,382 cm^{-1} is ascribed to the hydroxyl stretching vibration (Huang *et al.* 2008). Those at 1,654 cm^{-1} correspond to bending vibration of coordinated water molecules of O–H. The bands at 981 cm^{-1} are associated with the bending vibration of hydroxyl groups of metal oxides (M-OH) (Ding *et al.* 2014). The bands at 802 cm^{-1} are observed, which may be ascribed to the amorphous silica (Madejová 2003), whereas the bands at 452 cm^{-1} are related to Si-O-Si vibrations (Eren *et al.* 2009).

XRD spectra of NAC and HAC are depicted in Figure 2(b). According to XRD analyses, obvious peaks of quartz are detected in all the samples, indicating the main composition of the samples is quartz. No new peaks appear, nor do old peaks disappear. This result reveals no apparent differences among the crystal structure of samples, and the crystal structure of inner surface has not been broken after modification. Besides quartz, the main crystal compositions of the samples are diaspore and hematite. This observation is consistent with the previous study (Zhao *et al.* 2015).

In general, a higher value of BET provides a better contact between adsorbent and pollutants in the solution, which would result in a higher adsorption capacity. According to the BET test (Figure S1), the surface area of HAC (75.27 m^2/g) was smaller than that of NAC

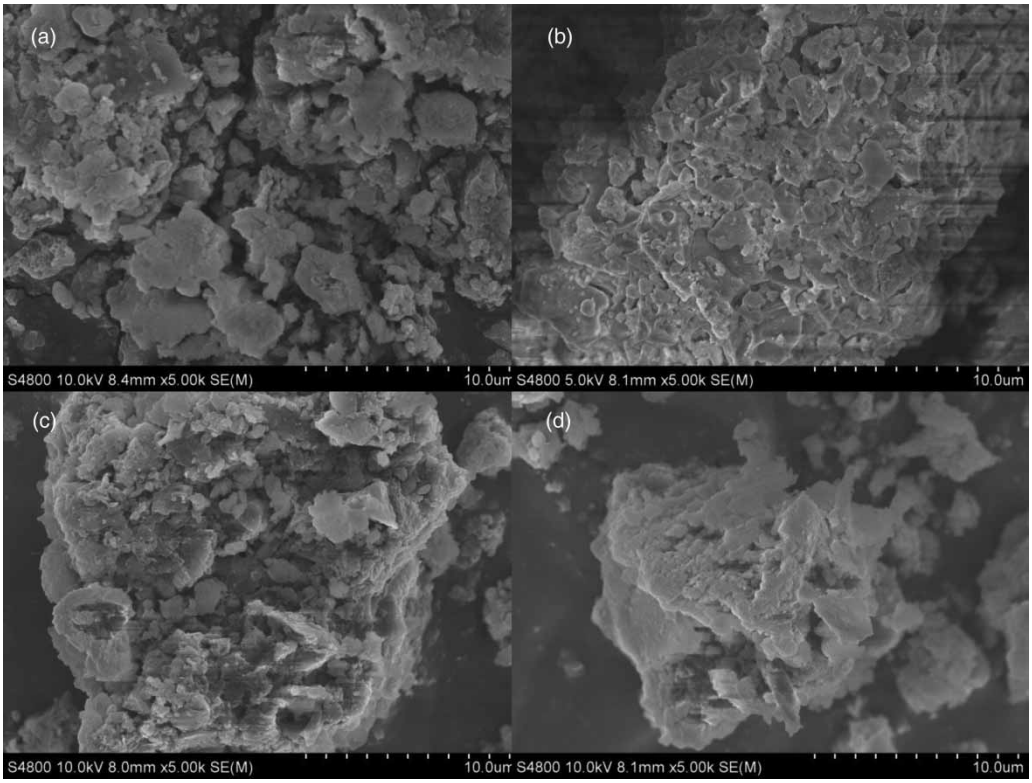

Figure 1 | SEM images (acceleration voltage: 5.0 kV and 5,000 magnification) of the NAC (a) and after phosphate adsorption (c), HAC (b) and after phosphate adsorption (d).

(117.67 m^2/g). However, HAC presented a little bit larger total pore volume (0.1597 m^3/g) than that of NAC (0.1359 m^3/g). Since partial impurities in the HAC were removed, especially in the mesopores, H^+ occupied and provided more active sites, resulting in a decrease in specific surface area and total pore volume after modification, which was in favor of the phosphate adsorption. The Barrett–Joyner–Halenda (BJH) pore size distribution of the NAC mostly varies between 1.43 and 100 nm. According to the International Union of Pure and Applied Chemistry (IUPAC) classification, NAC and HAC typically belong to mesoporous materials.

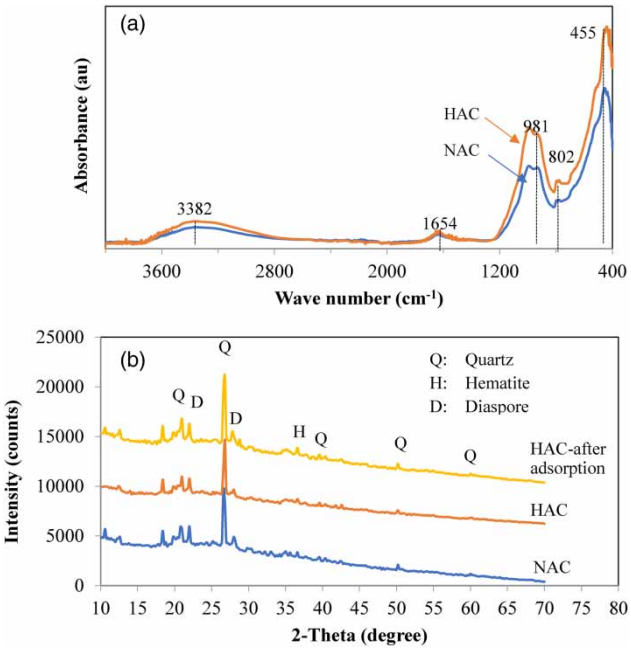

Figure 2 | FTIR (a) and XRD (b) spectra of the NAC and HAC.

Kinetic studies and effect of contact time

Adsorption rate is a key factor for evaluating the performance of an adsorbent material. Generally, due to the different physical and chemical characteristics, such as pore size and surface charge, different adsorbents have different balance times in the process of adsorption due to different adsorption mechanisms. The phosphate adsorption capacities onto NAC and HAC are shown in Figure 3(a). It is clear that the phosphate adsorption capacity increased rapidly during the first 30 min, and the modified AC achieved an obviously higher adsorption capacity (3.38 mg/g) than NAC (2.70 mg/g). After that, the phosphate adsorption increased more gently,

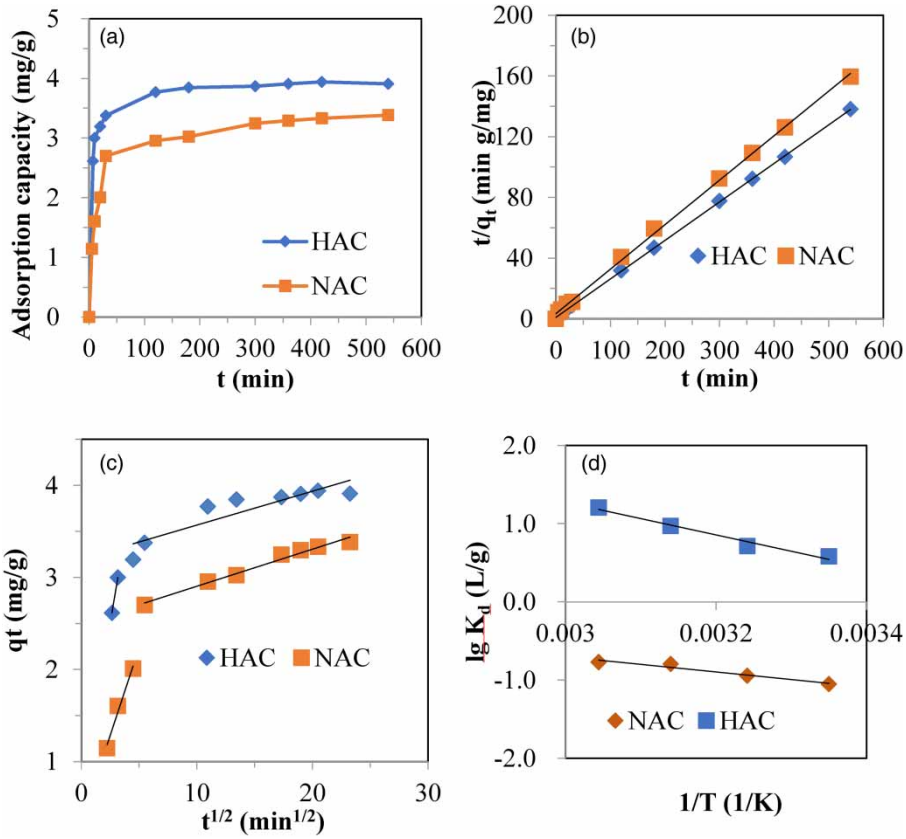

Figure 3 | Effect of contact time on phosphate removal by HAC and NAC (a), pseudo-second-order model (b), intra-particle diffusion equation (c), and thermodynamics (d) (contact time = 0–540 min, initial concentration = 20 mg/L, T = 25–55 °C).

and the adsorbents NAC and HAC reached saturation at 300 min and 180 min, achieving phosphate adsorption amount about 3.25 and 3.85 mg/g, respectively. Generally, HAC possessed a relatively higher adsorption capacity with a much shorter equilibrium time than NAC, demonstrating the superiority of the modified adsorbent material.

To elucidate the dynamics, the classical pseudo-first-order kinetic model (Lagergren 1898), pseudo-second-order kinetic model (Ho & McKay 1999), and intra-particle diffusion model (Weber & Morris 1962) were applied to investigate this kinetic process. The equations of the three models are expressed as follows, respectively.

$$\lg(q_e - q_t) = \lg q_e - \frac{k_1 t}{2.303} \quad (3)$$

$$\frac{t}{q_t} = \frac{1}{k_2 q_e^2} + \frac{t}{q_e} \quad (4)$$

$$q_t = k_{di} t^{1/2} + C_i \quad (5)$$

where q_e (mg/g) and q_t (mg/g) are the amount of phosphate adsorbed at equilibrium and time t (min), respectively. k_1 (1/min), k_2 (g/mg·min), and k_{di} (mg/g·min$^{1/2}$) are the rate constants of pseudo-first-order (Equation (3)), pseudo-second-order (Equation (4)), and intra-particle diffusion model (Equation (5)), respectively. C_i is the constant of intra-particle diffusion model. The values of q_e and k can be determined from the intercept and the slope of the linear plot of $lg(q_e\text{-}q_t)$ against t for the pseudo-first-order model and the plot of t/q_t against t for the pseudo-second-order model. The value of C_i and k_{di} can be determined from the intercept and slope of the linear plot of q_t against $t^{1/2}$.

The corresponding parameters and correlation coefficients are listed in Table 1. The correlation coefficients of NAC ($R^2 = 0.998$) and HAC ($R^2 = 0.999$) revealed that the adsorption kinetic data fitted better to the pseudo-second-order (Figure 3(b)) than the pseudo-first-order equation ($R^2 = 0.849$ for NAC, and $R^2 = 0.794$ for HAC) (Figure S2). In addition, the calculated equilibrium adsorption capacity data ($q_{e,cal}$) by the pseudo-second-order model were similar

Table 1 | The adsorption kinetic model constants and correlation coefficients of phosphate adsorption onto HAC and NAC

Model	parameters	HAC	NAC
	$q_{e.exp}$ (mg/g)	3.93	3.59
Pseudo-first-order	$q_{e.cal}$ (mg/g)	0.97	1.77
	k_1 (1/min)	0.008	0.005
	R^2	0.794	0.849
Pseudo-second-order	$q_{e.cal}$ (mg/g)	3.95	3.41
	k_2 (g/mg·min)	0.069	0.015
	R^2	0.999	0.998
Intra-particle diffusion	k_{d1} (mg/g·$min^{1/2}$)	0.745	0.381
	C_1	0.641	0.330
	R^2	1.000	0.982
	k_{d2} (mg/g·$min^{1/2}$)	0.036	0.040
	C_2	3.200	2.501
	R_2	0.813	0.980

with the experimental data ($q_{e,exp}$), further proving the feasibility of the pseudo-second-order model. This observation indicates that the adsorption process is a chemisorption, and the adsorption behavior might involve the valency variation or electrons sharing between phosphate ions and the adsorbent (Lalley *et al.* 2016).

The adsorption process comprises multiple steps, including the transport of molecule from the aqueous phase to the solid surface, and then intra-particle diffusion into the adsorbent pores. The intra-particle diffusion model can be used to clarify the mechanism of diffusion and to investigate the adsorption process whether particle diffusion is a rate limiting step. The two linear portions in Figure 3(c) indicate the multi-stage adsorption processes. It is known that if the lines pass through the origin in the first phase, then the adsorption rate is controlled by intra-particle diffusion. Otherwise, both *Ci* values of HAC and NAC are not zero and proportional to the boundary layer thickness, suggesting that there is an association of film diffusion with intra-particle diffusion (Lalley *et al.* 2016). The first phase is due to the external surface adsorption or transient adsorption driven by the initial phosphate concentration. The second phase is the equilibrium stage and the intra-particle diffusion rate begins to slow down ($k_{d1} > k_{d2}$), as the increment of occupied active sites in the limited space, the residual phosphate concentration in solution gradually becomes lower. Results from this work show that the intra-particle diffusion is the rate limiting step. And the k_{d1} of HAC was much greater than that of NAC, signaling that the adsorption rate of HAC was much higher than that of NAC, which was consistent with Figure 3(a).

Adsorption isotherm

The adsorption isotherm can reveal the specific relationship between the equilibrium adsorbate concentration in the bulk and the amount adsorbed on the surface. In this study, the adsorption isotherms were evaluated using Langmuir model and Freundlich model, which can be described as Equations (6) and (7), respectively (Freundlich 1907; Langmuir 1916). The Langmuir model is commonly used to demonstrate the monolayer distribution of adsorbate on the adsorbent, whereas the Freundlich adsorption isotherm model describes a heterogeneous adsorption process, assuming that different sites with several adsorption energies are complex (Su *et al.* 2011).

$$q_e = \frac{q_{max} b\, C_e}{1 + b\, C_e} \tag{6}$$

$$q_e = K_F C_e^{1/n} \tag{7}$$

where q_e is the amount of phosphate adsorbed on per unit weight of adsorbent (mg/g), C_e is the equilibrium solution phase concentration (mg /L), q_{max} and b are Langmuir constants related to the maximum adsorption capacity (mg/g) corresponding to complete coverage of available adsorption sites and energy of adsorption (L/mg), respectively. K_F and n are the Freundlich constants related to adsorption capacity ((mg/g)/$(mg/L)^{1/n}$) and intensity of adsorption, respectively. The results are shown in Figure S3 and Table 2. The higher R^2 of HAC and NAC ($R^2 = 0.964$ and 0.958, respectively) show a very good mathematical fit of the experimental data to the Langmuir isotherm model. A previous study also claimed that the Langmuir model showed a better fit to phosphate adsorption than the Freundlich model (Yan *et al.* 2015). This observation indicates that the phosphate adsorption onto HAC or NAC is a monolayer adsorption onto homogeneous surface and there is no interaction

Table 2 | The adsorption isotherm model parameters and correlation coefficients of phosphate adsorption onto HAC and NAC

Model	parameters	HAC	NAC
	$q_{e.exp}$ (mg/g)	9.02	6.09
Langmuir model	q_{max} (mg/g)	9.19	5.88
	b (L/mg)	0.871	0.632
	R^2	0.964	0.958
Freundlich model	K_F (mg/g)/$(mg/L)^{1/n}$	4.81	2.77
	n	5.441	5.112
	R^2	0.915	0.919

between sorbed molecules at the tested concentrations (Chen *et al.* 2010). The estimated monolayer maximum adsorption capacity (q_{max}) for the prepared HAC was determined to be higher (9.19 mg/g) than that of NAC (5.88 mg/g). In addition, the experimental value of HAC (9.02 mg/g) was close to this theoretical value. It is obvious that acid activation method could enhance adsorption abilities of akadama clay for phosphate removal. Table 3 compares the adsorption capacities obtained in this work with previous research works. It could be seen that the adsorption capacity of acid-activated akadama clay (HAC) is comparable to other adsorbents, implying its potential application for phosphate removal from wastewater.

Adsorption thermodynamics

The effect of temperature on the adsorption of phosphate was studied in the temperature range of 298.5–328.5 K (25–55 °C). The thermodynamic parameters related to the adsorption, standard Gibbs free energy ΔG, ΔH and ΔS were calculated according to Equation (8) and from the slope and intercept of the plot of $\ln K_d$ versus 1/T using Equation (9).

$$\Delta G = -RT\ln K_d \quad (8)$$

$$\ln K_d = \frac{\Delta S}{R} - \frac{\Delta H}{RT} \quad (9)$$

where ΔG (kJ/mol) is the standard free energy of adsorption, ΔH (kJ/mol) is the standard enthalpy change, ΔS (J/mol K) is the standard entropy change, T (K) is the absolute temperature of the phosphate solution, R (8.314 J/mol K) is the gas constant and K_d (mL/g) is the thermodynamic equilibrium constant.

The linear plot of $\ln K_d$ versus 1/T and the calculated values of thermodynamic parameters are shown in Figure 3(d) and Table 4. The positive values of ΔG indicated the nature of reaction of NAC is not spontaneous under the experimental condition, while that of HAC is a spontaneous process. In addition, with the increase in absolute temperature, ΔG showed a declining trend suggesting higher temperature is in favor of adsorption. The positive value of ΔH indicates that the adsorption process is endothermic, and the positive value of ΔS is relative to the increased disorder at the solid/solution interfaces during phosphate adsorption (Rajeswari *et al.* 2015).

Effects of dosage, pH and co-existing anions

It can be seen from Figure 4(a) that when the dosage was 2.5 g/L, both the phosphate removal efficiency and adsorption capacity of HAC (93%, 7.02 mg/g) were higher than those of NAC (52%, 3.73 mg/g), reflecting the successful modification process of NAC. With dosage ranged from 1.25–12.5 g/L, the phosphate removal efficiency increased with the increase in adsorbent dosage, suggesting that more available adsorption sites existed in the adsorbent to achieve higher removal efficiency. In addition, the adsorption capacity decreasing tendency was attributable to the lower utilization ratio of adsorption sites at higher dosage.

The pH of phosphate solution, a crucial factor influencing the properties of the adsorbent surface, on the adsorption of phosphate onto NAC and HAC could be seen from Figure 4(b). It was found that the phosphate removal efficiency of the NAC could be up to 94% with a adsorption capacity of 7.65 mg/g when pH was 3.00, while for HAC the similar removal efficiency and adsorption capacity could be stably achieved when pH ranged from 3.00–6.00. As for HAC obtained in this study, the

Table 3 | Comparison of phosphate adsorption capacities among various clay materials

Adsorbents	Adsorption capacity (mg/g)	References
Hydrous iron oxide modified diatomite	4.89–35.71	Wang *et al.* (2016)
Modified montmorillonite ($C_{1.0}$-AlPMt)	11.89	Ma *et al.* (2016)
Bentonite	5.54	Yan *et al.* (2010)
Magnetic illite clay	5.48	Chen *et al.* (2016)
Na-natural zeolite	2.19	Wu *et al.* (2006)
Sepiolite	0.60	Ooi *et al.* (2017)
Akadama clay	5.88	This study
Acid-activated akadama clay	9.19	This study

Table 4 | Thermodynamic parameters for phosphate adsorption onto HAC and NAC

Adsorbents	T (K)	K_d (mL/g)	ΔG (kJ/mol)	ΔS (J/mol•K)	ΔH (kJ/mol)
NAC	298.5	0.35	2.59	18.36	8.07
	308.5	0.39	2.40	18.36	8.07
	318.5	0.45	2.22	18.36	8.07
	328.5	0.46	2.04	18.36	8.07
HAC	298.5	1.79	−1.35	62.63	17.34
	308.5	2.04	−1.98	62.63	17.34
	318.5	2.64	−2.60	62.63	17.34
	328.5	3.35	−3.23	62.63	17.34

relationship between pH and adsorption capacity is similar to a previous report (Liu *et al.* 2011). It means that the pristine akadama clay could only be a potential effective adsorbent for phosphate under extremely acid conditions. It is well known that the actual pH in the most domestic wastewaters is generally neutral or near neutral (Wang *et al.* 2016). This result suggests that HAC developed in this study could be more applicable in the real world of wastewater treatment. The adsorption capacity, however, tended to decrease with the increase in solution pH, probably due to the competition for adsorption sites between phosphate and hydroxyl ions. The detailed illustration would be presented in the adsorption mechanisms section.

The adsorption affinity is often represented in terms of distribution coefficient, K_d (ml/g), which can be expressed as Equation (10) (Ji *et al.* 2015).

$$K_d = \frac{C_0 - C_e}{C_e} \times \frac{V}{M} \tag{10}$$

where C_0 and C_e are the initial and equilibrium concentrations of phosphate in the solution. V is the volume of solution (mL), and M is the amount of adsorbent (g).

The distribution coefficient changed with the pH value as shown in Figure 4(c). The best adsorption performance was obtained at pH 3.00 and pH 4.00 for NAC and HAC, respectively, which was consistent with the results of adsorption capacity. In general, after modification, the applicable pH for phosphate removal changed from extremely acidic condition to weak acidic or neutral conditions (pH 3.00–7.00).

On the other hand, there are various types of suspended solids and salts existing in the real wastewaters. The adsorption process would be greatly affected due to the high

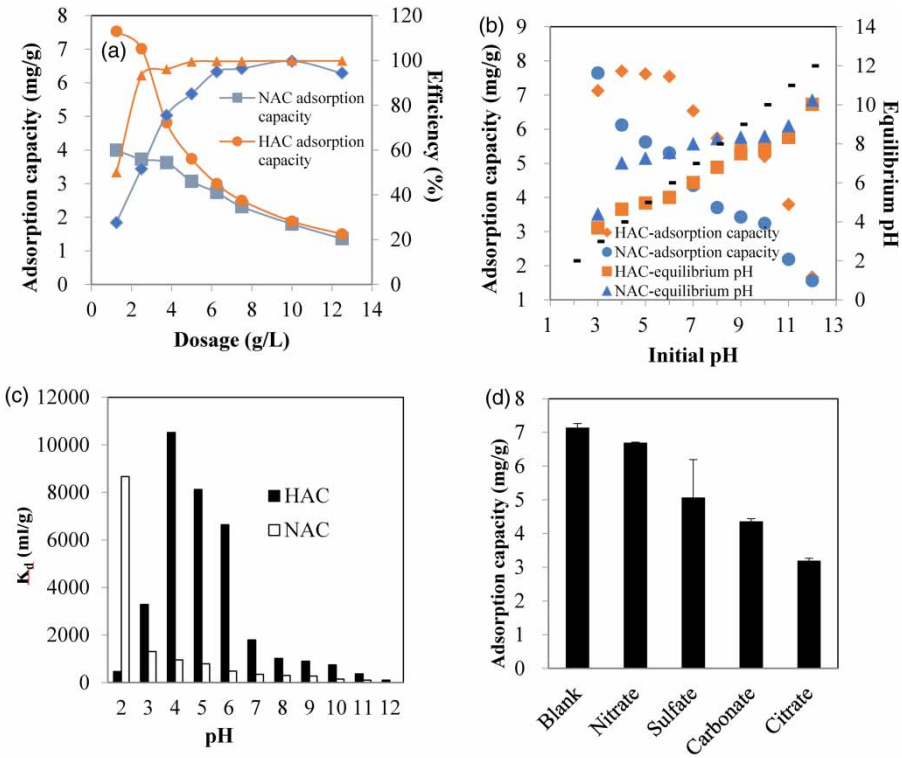

Figure 4 | Effects of dosage (a) and initial pH (b) on phosphate adsorption onto the NAC and HAC. Distribution coefficient of phosphate adsorption onto the NAC and HAC at different initial pH (c), and effect of coexisting anions on the phosphate adsorption by HAC (d). (Initial concentration = 20 mg/ L, dosage = 1.25–12.5 g/L, pH = 2.00–12.00, concentration of coexisting anions = 0.01 M).

ionic strength caused by coexisting ions. The common inorganic oxygen anions like nitrate, sulfate, carbonate were chosen in this study. Citrate, widely distributed in nature and mainly used for food additives and livestock husbandry, was examined as the representative of small organic anions. The results are presented in Figure 4(d). It is shown that addition of nitrate had negligible effect on the phosphate removal by HAC, while addition of sulfate and carbonate showed some negative effects. The inhibition of inorganic anions on phosphate adsorption followed the following descending order: $CO_3^{2-} > SO_4^{2-} > NO_3^-$, which have different molecular dimensions, charge density and hydration degree. As an organic anion, coexistence of citrate decreased the adsorption capacity of phosphate by 55%, indicating that small organic acid has a relatively strong competition effect against phosphate adsorption.

Adsorption mechanisms

As discussed previously, the phenomenon of different adsorption capacity under different pH may be caused by the acid–base surface properties of the adsorbent and phosphate species variation at different solution pH conditions. The point of zero charge (pH_{pzc}) is about 5.55 (Figure S3) for NAC and is 4.00 (Figure S4) for HAC by using the same method as a previous work (Zeng *et al.* 2011). The decrease in pH_{pzc} as the result of acidic treatment indicates an increase of the acidity of the AC surface (Lazarević *et al.* 2007). Some of the cations on the surface of the adsorbent are replaced by protons, resulting in more surface adsorption sites which are in favor of the capture of phosphates in the solution, which could also be supported by the BET results. The observation suggests that acid modification process plays an important role in surface charge behavior of the adsorbent.

At a lower pH and in the process of acid activating AC, the adsorbent surface could be protonated in accordance with the following reaction:

$$\equiv M - OH + H^+ \leftrightarrow \equiv M - OH_2^+ \tag{11}$$

At a higher pH, the adsorbent surface could be deprotonated as follows:

$$\equiv M - OH \leftrightarrow \equiv M - O^- + H^+ \tag{12}$$

where M represents Fe, Al, etc.

Therefore, phosphate sorption would become more favorable at lower pH than at higher pH. Moreover, phosphate dissociation equilibrium in aqueous solution is pH-related (Yang *et al.* 2013). In the pH range of 3.00–10.00, $H_2PO_4^-$ and HPO_4^{2-} are the predominant species. The adsorption free energy of $H_2PO_4^-$ is lower than that of HPO_4^{2-} (Lu *et al.* 2015), thus $H_2PO_4^-$ is more easily adsorbed on the adsorbent surface than HPO_4^{2-} at a lower pH.

As reported, AC contains silicon, iron and aluminum oxides. The ligand, -OH would bond with Si-O, Fe-O or Al-O bond (Xue *et al.* 2009). In the pH range of 3.00–5.00, the significant positive ΔpH (ΔpH = final pH − initial pH) indicates that ligand exchange ($H_2PO_4^-$ may exchange with hydroxyl groups (Si-OH, Fe-OH, Al-OH)) is one of the mechanisms for phosphate adsorption by HAC, resulting in the release of OH^- to the solution. Meanwhile, the adsorbent surface becomes protonated and positively charged ($Si\text{-}OH_2^+$, $Fe\text{-}OH_2^+$, $Al\text{-}OH_2^+$), which would more significantly attract the negatively charged phosphate anions $H_2PO_4^-$ and HPO_4^{2-}. The mechanism could also be explained by the electrostatic attraction between adsorbent and adsorbate (Chen *et al.* 2016). These mechanisms could be expressed as follows:

$$\equiv M - OH_2^+ + H_2PO_4^- \leftrightarrow (\equiv M - OH_2)^+(H_2PO_4)^- \tag{13}$$

$$\equiv M - OH + H_2PO_4^- \leftrightarrow \equiv MH_2PO_4^- + OH^- \tag{14}$$

$$\equiv 2M - OH + H_2PO_4^{2-} \leftrightarrow \equiv M_2HPO_4 + 2OH^- \tag{15}$$

However, it is observed that HAC had a significant capacity to buffer highly acidic and alkaline solutions. It could be proven by the different pH_{zpc} in Figures S4 and S5. During the measurement of pH_{pzc}, the final pH could be maintained at 5.80 for NAC (with initial pH from 5.00–9.00) and 4.20 for HAC (with initial pH from 4.00–9.00), respectively, indicating that HAC has stronger buffering capacity and is conducive to maintaining equilibrium pH. If the pH increases too much after adsorption, deprotonation of the adsorbent surface is not conducive to the contact of phosphate with the adsorbent surface. Therefore, HAC is more favorable for Equations (14) and (15) to proceed in the positive direction. As for HAC, when pH (pH = 5.00–12.00) is greater than pH_{zpc}, phosphate adsorption by electrostatic attraction may gradually weaken due to the deprotonation, leading to the decrease of adsorption capacity. At the same time, a strong electrostatic repulsion becomes more dominant, which prevents $HPO_4^{2-}$and PO_4^{3-} from approaching the surface of adsorbent. For NAC,

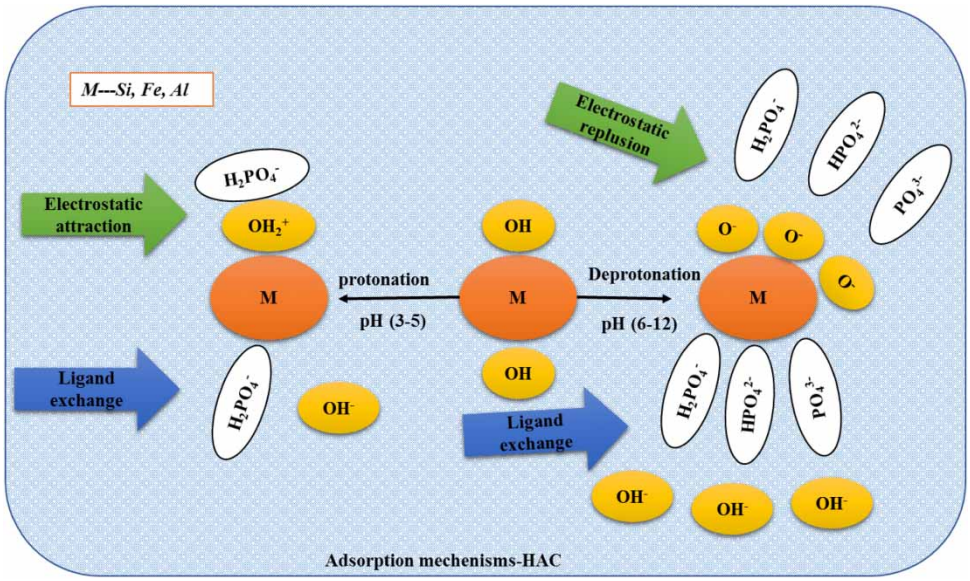

Figure 5 | Proposed mechanisms for the removal of phosphate onto HAC at different initial solution pHs.

when the pH was elevated from 3.00 to 12.00, the phosphate adsorption capacity was decreased from 7.65 mg/g to 1.56 mg/g. The suitable pH range of NAC is relatively narrow and could only exhibit higher adsorption capacity under extremely acidic pH conditions. The surface of HAC seems to have more protons with enhanced electrostatic attraction. Moreover, its negative Gibbs free energy implies the necessity of acid treatment.

In summary, as proposed in Figure 5, the mechanisms involved in the adsorption process of phosphate by HAC include electrostatic attraction and ligand exchange, and the major mechanism may vary with the solution pH.

CONCLUSIONS

Acid-activated akadama clay exhibited excellent phosphate adsorption ability, indicating that acid modification is a feasible method to improve the phosphorus adsorption capacity of clay materials. The adsorption process was pH-dependent and reached equilibrium within 300 min or 180 min for natural akadama clay and acid-activated akadama clay, respectively. Compared with the highest adsorption capacity of the natural akadama clay achieved from extremely acidic phosphate solution (pH = 3.00), the acid-activated akadama clay shows the advantage of being suitable for treating weak acidic to neutral phosphate-containing wastewater (pH = 3.00–6.00). The adsorption kinetics followed the pseudo-second-order kinetic model and the rate-limiting step was influenced by intra-particle diffusion. The experimental data well fitted Langmuir isotherm model with the maximum adsorption capacity of natural akadama clay and acid-activated akadama clay being 5.88 and 9.19 mg/g, respectively. According to the thermodynamic test, the phosphate removal onto the acid-activated akadama clay was a spontaneous and endothermic process, reflecting a promising adsorbent for real wastewater treatment. The mechanisms were interpreted by electrostatic attraction and ligand exchange, depending on the solution pH. Further studies are necessary to test the efficiency of acid-activated akadama clay in treating real wastewater by using fixed-bed columns and its feasibility in real wastewater treatment plants, and to apply the P loaded acid-activated akadama clay as soil fertilizer as well. The data will be fitted to the physical models to observe the interferences from other anions. In addition, how to further enhance the adsorption selectivity towards phosphate by this kind of adsorbent is also demanding.

ACKNOWLEDGEMENTS

The first author acknowledges the support of the China Scholarship Council (No. 201608050104). The authors wish to thank Mr. Jiang Yong for the analysis of data. This research did not receive any specific grant from funding agencies in the public, commercial, or not-for-profit sectors.

REFERENCES

Chen, R., Zhang, Z., Feng, C., Lei, Z., Li, Y., Li, M., Shimizu, K. & Sugiura, N. 2010 Batch study of arsenate (V) adsorption using Akadama mud: effect of water mineralization. *Applied Surface Science* **256** (9), 2961–2967.

Chen, J., Yan, L. G., Yu, H. Q., Li, S., Qin, L. L., Liu, G. Q., Li, Y. F. & Du, B. 2016 Efficient removal of phosphate by facile prepared magnetic diatomite and illite clay from aqueous solution. *Chemical Engineering Journal* **287**, 162–172.

Diaz, R. J. & Rosenberg, R. 2008 Spreading dead zones and consequences for marine ecosystems. *Science* **321** (5891), 926–929.

Ding, D., Lei, Z., Yang, Y. & Zhang, Z. 2014 Efficiency of transition metal modified akadama clay on cesium removal from aqueous solutions. *Chemical Engineering Journal* **236**, 17–28.

Eren, E., Afsin, B. & Onal, Y. 2009 Removal of lead ions by acid activated and manganese oxide-coated bentonite. *Journal of Hazardous Materials* **161** (2–3), 677–685.

Freundlich, H. 1907 Über die Adsorption in Lösungen. *Zeitschrift für Physikalische Chemie* **57** (1), 385–470.

Henze, M., Van Loosdrecht, M., Ekama, G. A. & Brdjanovic, D. 2008 *Biological Wastewater Treatment: Principles, Modelling and Design*. IWA Publishing, London, UK.

Ho, Y. S. & McKay, G. 1999 Pseudo-second-order model for sorption processes. *Process Biochemistry* **34** (5), 451–465.

Huang, W., Wang, S., Zhu, Z., Li, L., Yao, X., Rudolph, V. & Haghseresht, F. 2008 Phosphate removal from wastewater using red mud. *Journal of Hazardous Materials* **158** (1), 35–42.

Ji, M., Su, X., Zhao, Y., Qi, W., Wang, Y., Chen, G. & Zhang, Z. 2015 Effective adsorption of Cr(VI) on mesoporous Fe-functionalized Akadama clay: optimization, selectivity, and mechanism. *Applied Surface Science* **344**, 128–136.

Lagergren, S. 1898 About the theory of so-called adsorption of soluble substance. *Sven. Vetenskapsakad. Handingarl* **24**, 1–39.

Lalley, J., Han, C., Li, X., Dionysiou, D. D. & Nadagouda, M. N. 2016 Phosphate adsorption using modified iron oxide-based sorbents in lake water: kinetics, equilibrium, and column tests. *Chemical Engineering Journal* **284**, 1386–1396.

Langmuir, I. 1916 The constitution and fundamental properties of solids and liquids. Part I. Solids. *Journal of the American Chemical Society* **38** (11), 2221–2295.

Lazarević, S., Janković-Častvan, I., Jovanović, D., Milonjić, S., Janaćković, D. & Petrović, R. 2007 Adsorption of Pb^{2+}, Cd^{2+} and Sr^{2+} ions onto natural and acid-activated sepiolites. *Applied Clay Science* **37** (1–2), 47–57.

Liu, J., Wan, L., Zhang, L. & Zhou, Q. 2011 Effect of pH, ionic strength, and temperature on the phosphate adsorption onto lanthanum-doped activated carbon fiber. *Journal of Colloid and Interface Science* **364** (2), 490–496.

Lu, J., Liu, D., Hao, J., Zhang, G. & Lu, B. 2015 Phosphate removal from aqueous solutions by a nano-structured Fe-Ti bimetal oxide sorbent. *Chemical Engineering Research and Design* **93**, 652–661.

Ma, L., Zhu, J., Xi, Y., Zhu, R., He, H., Liang, X. & Ayoko, G. A. 2016 Adsorption of phenol, phosphate and Cd(II) by inorganic-organic montmorillonites: A comparative study of single and multiple solute. *Colloids and Surfaces A: Physicochemical and Engineering Aspects* **497**, 63–71.

Madejová, J. 2003 FTIR techniques in clay mineral studies. *Vibrational Spectroscopy* **31** (1), 1–10.

Novaković, T., Rožić, L., Petrović, S. & Rosić, A. 2008 Synthesis and characterization of acid-activated Serbian smectite clays obtained by statistically designed experiments. *Chemical Engineering Journal* **137** (2), 436–442.

Ooi, K., Sonoda, A., Makita, Y. & Torimura, M. 2017 Comparative study on phosphate adsorption by inorganic and organic adsorbents from a diluted solution. *Journal of Environmental Chemical Engineering* **5** (4), 3181–3189.

Rajeswari, A., Amalraj, A. & Pius, A. 2015 Removal of phosphate using chitosan-polymer composites. *Journal of Environmental Chemical Engineering* **3** (4), 2331–2341.

Su, J., Huang, H. G., Jin, X. Y., Lu, X. Q. & Chen, Z. L. 2011 Synthesis, characterization and kinetic of a surfactant-modified bentonite used to remove As(III) and As(V) from aqueous solution. *Journal of Hazardous Materials* **185** (1), 63–70.

U.S. Environmental Protection Agency. 1996 *Quality Criteria for Water*.

Wang, Z., Lin, Y., Wu, D. & Kong, H. 2016 Hydrous iron oxide modified diatomite as an active filtration medium for phosphate capture. *Chemosphere* **144**, 1290–1298.

Weber, W. J. & Morris, J. C. S. 1962 Advances in Water Pollution Research: Proceedings of the International Conference. In: *Pergamon Press*, Oxford, UK, pp. 231–266.

Wu, D., Zhang, B., Li, C., Zhang, Z. & Kong, H. 2006 Simultaneous removal of ammonium and phosphate by zeolite synthesized from fly ash as influenced by salt treatment. *Journal of Colloid and Interface Science* **304** (2), 300–306.

Xu, K., Deng, T., Liu, J. & Peng, W. 2010 Study on the phosphate removal from aqueous solution using modified fly ash. *Fuel* **89** (12), 3668–3674.

Xue, Y., Hou, H. & Zhu, S. 2009 Characteristics and mechanisms of phosphate adsorption onto basic oxygen furnace slag. *Journal of Hazardous Materials* **162** (2–3), 973–980.

Yan, L. G., Xu, Y. Y., Yu, H. Q., Xin, X. D., Wei, Q. & Du, B. 2010 Adsorption of phosphate from aqueous solution by hydroxy-aluminum, hydroxy-iron and hydroxy-iron-aluminum pillared bentonites. *Journal of Hazardous Materials* **179** (1–3), 244–250.

Yan, L. G., Yang, K., Shan, R. R., Yan, T., Wei, J., Yu, S. J., Yu, H. Q. & Du, B. 2015 Kinetic, isotherm and thermodynamic investigations of phosphate adsorption onto core-shell Fe_3O_4@LDHs composites with easy magnetic separation assistance. *Journal of Colloid and Interface Science* **448**, 508–516.

Yang, S., Ding, D., Zhao, Y., Huang, W., Zhang, Z., Lei, Z. & Yang, Y. 2013 Investigation of phosphate adsorption from aqueous solution using Kanuma mud: behaviors and mechanisms. *Journal of Environmental Chemical Engineering* **1** (3), 355–362.

Ye, J., Cong, X., Zhang, P., Zeng, G., Hoffmann, E., Liu, Y., Wu, Y., Zhang, H., Fang, W. & Hahn, H. H. 2016 Application of acid-activated Bauxsol for wastewater treatment with high phosphate concentration: characterization, adsorption optimization, and desorption behaviors. *Journal of Environmental Management* **167**, 1–7.

Zeng, F., Liu, W.-J., Luo, S.-W., Jiang, H., Yu, H. & Guo, Q. 2011 Design, preparation, and characterization of a novel hyper-cross-linked polyphosphamide polymer and its adsorption for phenol. *Industrial & Engineering Chemistry Research* **50** (20), 11614–11619.

Zhao, Y., Qi, W., Chen, G., Ji, M. & Zhang, Z. 2015 Behavior of Cr (VI) removal from wastewater by adsorption onto HCl activated Akadama clay. *Journal of the Taiwan Institute of Chemical Engineers* **50**, 190–197.

First received 31 March 2018; accepted in revised form 5 October 2018. Available online 15 October 2018